*mathematics*

MDPI

*Article*

# Bulk Low-Inertia Power Systems Adaptive Fault Type Classification Method Based on Machine Learning and Phasor Measurement Units Data

**Mihail Senyuk [1], Svetlana Beryozkina [2], Inga Zicmane [3,*], Murodbek Safaraliev [1], Viktor Klassen [1] and Firuz Kamalov [4]**

[1] Department of Automated Electrical Systems, Ural Federal University, 620002 Yekaterinburg, Russia; mdseniuk@urfu.ru (M.S.); murodbek_03@mail.ru (M.S.); viktor.klassen@urfu.me (V.K.)
[2] College of Engineering and Technology, American University of the Middle East, Kuwait; svetlana.berjozkina@aum.edu.kw
[3] Faculty of Electrical and Environmental Engineering, Institute of Industrial Electronics, Electrical Engineering and Energy, Riga Technical University, Azenes Street 12/1, LV-1048 Riga, Latvia
[4] Department of Electrical Engineering, Canadian University Dubai, Dubai 117781, United Arab Emirates; firuz@cud.ac.ae
* Correspondence: inga.zicmane@rtu.lv

**Abstract:** This research focuses on developing and testing a method for classifying disturbances in power systems using machine learning algorithms and phasor measurement unit (PMU) data. To enhance the speed and accuracy of disturbance classification, we employ a range of ensemble machine learning techniques, including Random forest, AdaBoost, Extreme gradient boosting (XGBoost), and LightGBM. The classification method was evaluated using both synthetic data, generated from transient simulations of the IEEE24 test system, and real-world data from actual transient events in power systems. Among the algorithms tested, XGBoost achieved the highest classification accuracy, with 96.8% for synthetic data and 85.2% for physical data. Additionally, this study investigates the impact of data sampling frequency and calculation window size on classification performance. Through numerical experiments, we found that increasing the signal sampling rate beyond 5 kHz and extending the calculation window beyond 5 ms did not significantly improve classification accuracy.

**Keywords:** power system; power system faults; bus voltage; fault simulation; fault detection; machine learning; classification; phasor measurement units; digital signal processing; phasor data concentrator; emergency control; short-circuit current; power grid

**MSC:** 68T01



Academic Editor: Carlos Llopis-Albert

Received: 12 November 2024
Revised: 17 December 2024
Accepted: 17 January 2025
Published: 19 January 2025

**Citation:** Senyuk, M.; Beryozkina, S.; Zicmane, I.; Safaraliev, M.; Klassen, V.; Kamalov, F. Bulk Low-Inertia Power Systems Adaptive Fault Type Classification Method Based on Machine Learning and Phasor Measurement Units Data. *Mathematics* **2025**, *13*, 316. https://doi.org/10.3390/math13020316



## 1. Introduction

The key trends in the development of modern electric power systems (EPS) include the widespread adoption of digital devices for recording, collecting, and analyzing electrical parameters [1,2], the accelerated integration of renewable energy sources (RES) [3–7], and the expansion of permissible operating conditions enabled by digital monitoring systems and adaptive control [8–11]. A notable characteristic of modern EPS is the reduction in system inertia, resulting from the growing share of RES alongside the retirement of fossil fuel power plants. This reduction in inertia leads to faster transient processes and diminishes the effectiveness of emergency control systems.

The greatest impact of changes in the parameters of transient processes in EPS is reflected in the operation of emergency control (EC) systems, providing dynamic stability (TS). The triggering factor for the operation of these types of automation is the signal of the fact and type of short circuit (SC). The traditional method for determining the SC type is associated with the analysis of oscillograms of instantaneous current and voltage values [12–15] through the use of digital signal processing (DSP) methods, which implement calculations on a calculation window of several periods of industrial frequency [16]. In [17], it was shown that for modern EPS with a reduced inertia value, determining the parameters of the electrical mode and the fact of disturbance with a time delay corresponding to several periods of industrial frequency can lead to a decrease in the accuracy of the operation of EC devices and emergency control in general [18–23].

Today, one of the tools that can provide the identified requirements for EC systems is the machine learning (ML) method. This class of methods is actively used for the following tasks that arise during the operation of EPS:

- Forecasting power consumption [24,25];
- Forecasting the output power RES [26–29];
- Assessment of the technical condition of equipment [30–32];
- EPS stability assessment [33–37];
- EPS EC [38–42].

ML methods make it possible to achieve high performance and adaptability through the use of non-deterministic approaches to data analysis without reference to the mathematical model protected by EPS [43].

Determining the SC type based on synchronized vector measurements can be considered a classification problem with restrictions on the permissible time delay. Today, an effective solution to problems of this class can be performed on the basis of ML algorithms [44], which make it possible to achieve high performance and adaptability through the use of non-deterministic approaches to data analysis without reference to the mathematical model protected by EPS. The use of ML methods makes it possible to identify implicit correlations in data, ensure adaptability and additional training during operation [45]. These advantages of using ML algorithms in combination with synchronized vector measurements [46] allow the development of an accelerated SC-type identification method intended for use as a trigger for EC, providing EPS stability with reduced inertial component values.

The SC-type identification algorithm can be implemented using a phasor data concentrator (PDC) [47,48], which combines and processes data from several PMUs. This approach makes it possible to ensure redundancy of measurements characterizing the SC-type, which allows for adaptability and variability in solving the classification problem.

The methodology proposed in the article is intended primarily for emergency automation to ensure the stability of power systems, for which the type of SC (single-phase to ground, phase-to-phase, two-phase-ground, and three-phase to ground) has a greater influence. The problem of determining damaged phases is not considered in this study and is an area for future research.

The scientific novelty of the research lies in the development of an adaptive method for assessing the SC type based on machine learning algorithms, taking into account the redundancy of measurements and the flexibility of using existing measurements. On the other hand, the scientific novelty of the research is determined by a flexible method for determining the location of disturbances in EPS based on measurement redundancy and determining the requirements for measuring systems and DSP algorithms.

## 2. Power Systems SC Classification: State-of-the-Art Review

SC type definition refers to a multiclass supervised classification problem in which a probabilistic estimate of the type of disturbance must be determined from an input set of features. In this work, one of the following SCs is considered a disturbance type: three-phase to ground, single-phase to ground, phase-to-phase, two-phase to ground. The SC type identification task involves the use of hybrid algorithms that combine the approaches of digital signal processing DSP [49] and ML methods.

The following ML methods have been used to solve the SC type identification problem:

- K–nearest neighbors algorithm (KNN) [50];
- Support vector machine (SVM) [51,52];
- Decision tree (DT) [53];
- Fuzzy logic (FL) [54];
- Artificial neural network (ANN) [55];
- Probabilistic neural network (PNN) [56];
- Convolutional neural network (CNN) [57];
- Deep learning (DL) [58,59].

Among the ML methods for multiclass classification, one of the most interpretable is KNN. This method was developed in 1951 by E. Fix and D. Lawson [60]. The method is based on the procedure for calculating the distance from the analyzed data instance to the objects of the training sample. Classification of the analyzed data instance is performed by determining the most frequently occurring class in the array of shortest distances. The advantages of the KNN method include resistance to outliers and the ability to graphically interpret the results of the algorithm. The disadvantages of the method include high requirements for computing power due to the need to use the entire volume of the data sample for classification and low classification speed due to the need to repeatedly calculate the distance to selected elements of the data sample.

The authors of the study [50] proposed a method for identifying and classifying SCs in electrical networks for further use in distance protection. The method proposed by the authors uses a sliding calculation window with a width of half a period of industrial frequency, in which the root mean square value of the instantaneous current signals is calculated, followed by checking the disturbance identification criterion using the KNN method. To test the proposed method, the results of modeling transient processes for a five-node EPS test model in Matlab Simulink with a numerical integration step corresponding to a signal sampling frequency of 10 kHz are used. In a series of numerical experiments, the accuracy of the algorithm was 98% with an average time delay of 15 ms (10 ms calculation window and 5 ms calculation delay).

The SVM algorithm was developed by V. Vapnik and his colleagues in 1995 [61]. To solve the classification problem, the SVM algorithm constructs a separating hyperplane in a multidimensional feature space. The advantages of the SVM algorithm include its universality due to the possibility of using kernels of varying degrees of nonlinearity, its operating efficiency in high-dimensional spaces, and also the fact that the SVM algorithm is based on the problem of convex quadratic programming, which ensures the uniqueness of the solution. Among the disadvantages of the algorithm are its instability to noise in the source data and lack of a kernel selection algorithm.

In [51], the SVM algorithm was used to identify and classify the SC type. The proposed method for analyzing the type of disturbance in EPS uses a sliding calculation window of 0.25 s. in which instantaneous values of currents and voltages are recorded and then used as features for the SVM algorithm. To form a data sample, the results of a numerical simulation of a series of transient processes in the EPS IEEE9 model were used. The total data sample size was 25,168 scenarios with different types of SC and various parameters of

the electrical mode of the test EPS. In a series of experiments, the accuracy of the proposed method was 99.98%.

The authors of the study [52] also used the SVM algorithm to identify and classify the SC type in electrical networks. The proposed technique consists of using the results of applying the discrete wavelet transform (DWT) to instantaneous values of currents and voltages as features for SVM. To test the proposed method, a two-machine EPS test model was used, with a sampling frequency of instantaneous currents and voltages of 200 kHz. The average SC type identification error was less than 3% with an average delay of 0.3 s.

The DT algorithm is a tree-based piecewise constant approximation algorithm [62–64], the purpose of which is to form a system of rules aimed at identifying a data object for the class being taken into account. The advantages of the algorithm include high interpretability, the ability to use numerical and categorical data, and low requirements for computing power. Among the disadvantages of the DT algorithm are its tendency to overfit, possible instability of work, and the lack of an absolute guarantee of convergence.

To identify the SC type, a study [53] developed a technique that involved using the results of applying a discrete Fourier transform (DFT) with instantaneous current and voltage signals as features for the DT algorithm. To form a data sample, the results of the numerical simulation of disturbances in a two-machine EPS implemented in Matlab Simulink were used. The sampling frequency of instantaneous current and voltage signals during the simulation was chosen to be 20 kHz. The total data sample size was 2000 scenarios. For the considered EPS test model, the average delay of the proposed SC type identification technique was 30 ms with an accuracy of 100%.

The theory of fuzzy logic was proposed by L. Zadeh in 1965; according to this theory, the function of membership of a data instance to a class is not a discrete function taking the value 0 or 1, but continuous on the interval [0, 1] [65]. Fuzzy sets can be represented through ANN. In this case, the membership function is interpreted through the activation function, and the logical connections of the fuzzy set as special types of neurons. The advantages of fuzzy logic include its reliability, high flexibility, and low requirements for computing resources. Among the disadvantages of this approach are its inability to always ensure acceptable accuracy, the lack of an algorithm for constructing fuzzy systems, and the complexity of testing and debugging.

In [54], a combined approach was used to determine the type of SC, combining the theory of fuzzy logic and DWT. Instantaneous current signals are used as input data, to which DWT with Meyer wavelet is applied. To test the proposed methodology, a two-machine model with a voltage class of 230 kV was used; the sampling frequency of instantaneous currents and voltages was chosen equal to 10 kHz. Testing was performed for different types of SCs simulated on different sections of the considered transmission line. The SC type identification accuracy was 100% with an average time delay of 2 ms.

The beginning of ANN theory dates back to the early 1949s [66–69]. The development of computer technology and the theory of optimization and statistics has led to the active implementation of ANN. In particular, the depth of networks increased, and new configurations appeared.

In the study [55], ANN was used to identify the SC type. A two-machine EPS implemented in Matlab Simulink was used as a test model; the data sampling frequency was chosen to be 1 kHz. Pre-emergency and emergency instantaneous values of currents and voltages were used as input data. The total volume of the generated data sample was 7920 scenarios. During numerical experiments, an accuracy of 78.1% was achieved.

The authors of [56] proposed a method for identifying the SC type based on PNN. The authors highlight the following advantages of this type of ANN: no need to train on large amounts of data, higher accuracy compared to classical neural networks, and a

more suitable structure for solving the classification problem. The results of applying DWT with the Meyer wavelet to instantaneous current and voltage signals were used as initial data. The methodology was tested on a two-node EPS model. During testing, an average classification accuracy of 100% was obtained.

The study [57] proposed the use of CNN to identify SC type in electrical networks. This type of neural network uses a combination of convolutional layers and subsampling layers to recognize patterns in the source data. To train and test the proposed methodology, records of disturbances in the power system of the Association of Southeast Asian Nations in the period from 17 May 2017 to 17 January 2018 were used. The total data sample size was 12,894 scenarios. The accuracy obtained during testing was 100%.

Studies [58,59] used deep ANNs for SC type classification. The study [58] uses the results of applying the Hilbert-Huang transform to instantaneous current and voltage signals as input to an ANN. A two-node model was used for testing; the total data sample size was 3424 scenarios. The minimum classification accuracy on test data were 99.6%. A study was also carried out of the influence of noise in the source data, distributed generation and changes in the configuration of the electrical network on the result of classification of the type of disturbance.

The authors of [59] also used deep ANN in combination with DWT, applied to instantaneous current and voltage values, to identify the SC type. The data sample was formed as a result of modeling a series of transient processes in a test two-machine EPS at a data sampling frequency of 20 kHz. During testing, the effectiveness of the proposed SC type identification technique was shown in the presence of noise in the source data and changes in the parameters of the protected EPS.

Table 1 provides an analysis of the reviewed ML methods used for SC type identification. In Table 1, the symbol «–» indicates the absence of data.

**Table 1.** Analysis of ML algorithms used for SC type identification.

| Algorithm | Time Delay, ms | Accuracy, % | Merits | Drawbacks |
|---|---|---|---|---|
| KNN [50] | 15 | 98.00 | Resistance to outliers, the ability to graphically interpret the results of the algorithm. | High sensitivity to minor variations can lead to overfitting. |
| SVM [51,52] | 250 | 99.98 | Versatility, reliability, efficiency in large-dimensional spaces. | High sensitivity to minor variations can lead to overfitting. |
| | 300 | 97.00 | | |
| DT [53] | 30 | 100.00 | High interpretability, ability to use numeric and categorical data, low computing power requirements. | |
| FL [54] | 2 | 100.00 | Reliability, high flexibility, low requirements for computing resources. | |
| ANN [55] | – | 78.10 | High performance, ability to process noisy data, fault tolerance. | The need for a large data sample and high classification accuracy indirectly indicates retraining of algorithms. |
| PNN [56] | – | 100.00 | | |
| CNN [57] | – | 100.00 | | |
| DL [58,59] | 210 | 99.60 | | |
| | 20 | 99.70 | | |

Based on the analysis of the reviewed studies on SC type identification methods, the following conclusions can be drawn: most studies utilize simple two-node EPS test

models; they do not address the determination of the optimal calculation window size or the sampling frequency of the input data. Additionally, the issue of retraining the machine learning models used is not considered by the authors of these studies.

To overcome the shortcomings of the studies reviewed, more complex EPS models can be used in combination with the following ensemble ML algorithms: Random forest (RF) [70], Adaptive boosting (AdaBoost) [71], Extreme gradient boosting (XGBoost) [72], Light gradient boosted machine (LightGBM) [73].

An ensemble algorithm is understood as an algorithm that combines the results of individual simple algorithms [74]. This algorithm structure makes it possible to effectively combat the problem of overfitting and ensure high performance of algorithms due to the possibility of using parallel calculations.

## 3. Power Systems SC Classification Method

Identification of the SC type is based on the analysis of data received from the PMU installed in the nodes of the EPS fragment in question. The implementation of the methodology presented in the work is possible on the basis of PDC, which ensures the collection and primary processing of signals received from the PMU. To determine the composition of the input data for the classification task, the approach of determining nodes near the SC location is used. Individual criteria for classifying an SC as nearby for each EPS are given in Table 2. For the classification task, the amplitudes and phases of voltages of nodes nearby to the SC location are used, as well as the values of the amplitudes and phases of currents along connections departing from the selected nodes. This approach provides redundancy of information, which introduces additional degrees of freedom when solving the classification problem with ML algorithms. The technique of identifying nodes near the SC location also increases the speed of the classification procedure due to a reduction in the dimension of the problem being solved.

**Table 2.** Criteria for classifying SC as nearby.

| № | SC Type | Criterion: Positive Sequence Voltage Value |
|---|---|---|
| 1 | Three-phase | Less than 0.60 p.u. |
| 2 | Phase-to-phase | Less than 0.70 p.u. |
| 3 | Two-phase to ground | Less than 0.75 p.u. |
| 4 | Single phase | Less than 0.80 p.u. |

The criteria presented in Table 2 primarily depend on SC current levels, which are influenced by the electrical network topology, the number of transformers with grounded neutrals, the number of synchronous generators (SGs) connected to the network, and the motor load. Recalculating the criteria requires a series of electromagnetic transient analyses to account for changes in network topology, the number of SGs, motor load, and transformer neutral operating modes. This process can be automated by pre-calculating SC locations and types based on parameter changes within the EPS mathematical model. Automating the update of the criteria in Table 2 is an essential task, which will be addressed in future studies.

Figure 1 illustrates the methodology for selecting SC nodes near the location. Figure 1 shows the numbered EPS nodes, the red arrow indicates the SC location, the nodes nearby to the SC location are highlighted in gray, and next to each node there is a PMU device from which data are sent to the PDC.

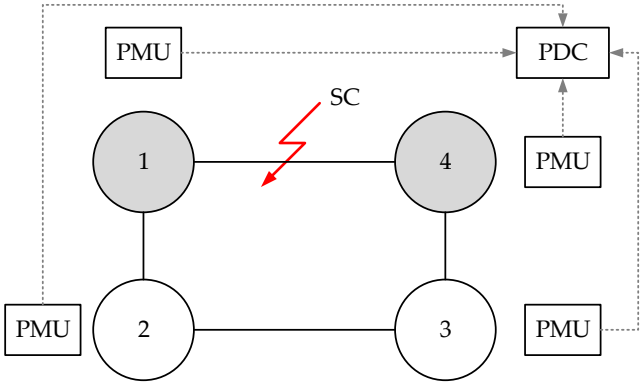


**Figure 1.** Illustrations of the technique for selecting nodes nearby to the SC site.

In this study, the criteria for classifying SC as nearby were obtained through a series of numerical experiments in the IEEE24 digital model. To classify the SC type, a two-stage technique was employed, intended for use in the operational control loop of EPS modes. A block diagram of the proposed methodology for training an ML method is presented in Figure 2. Figure 3 shows a block diagram of applying the trained ML method for emergency control of EPS modes.

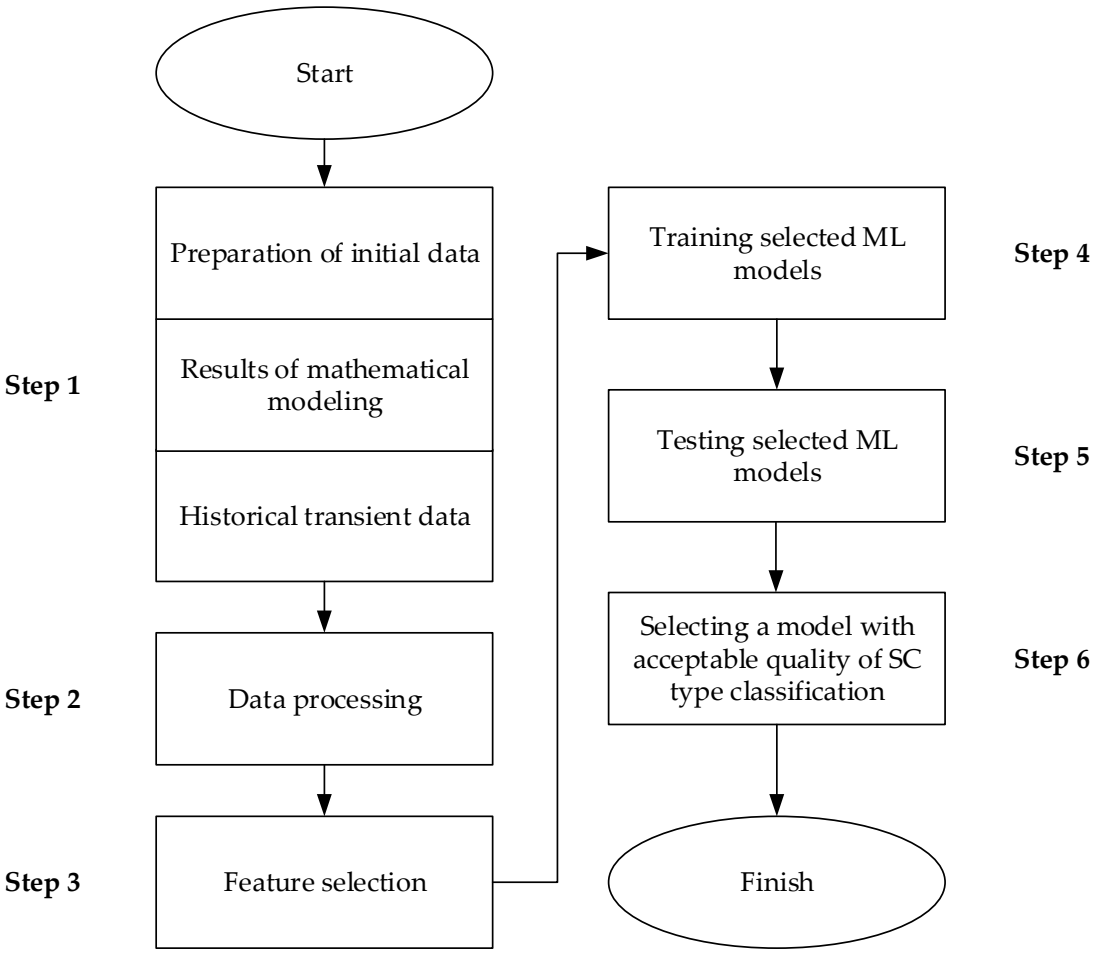


**Figure 2.** Flowchart for training methodology of ML method for SC identification.

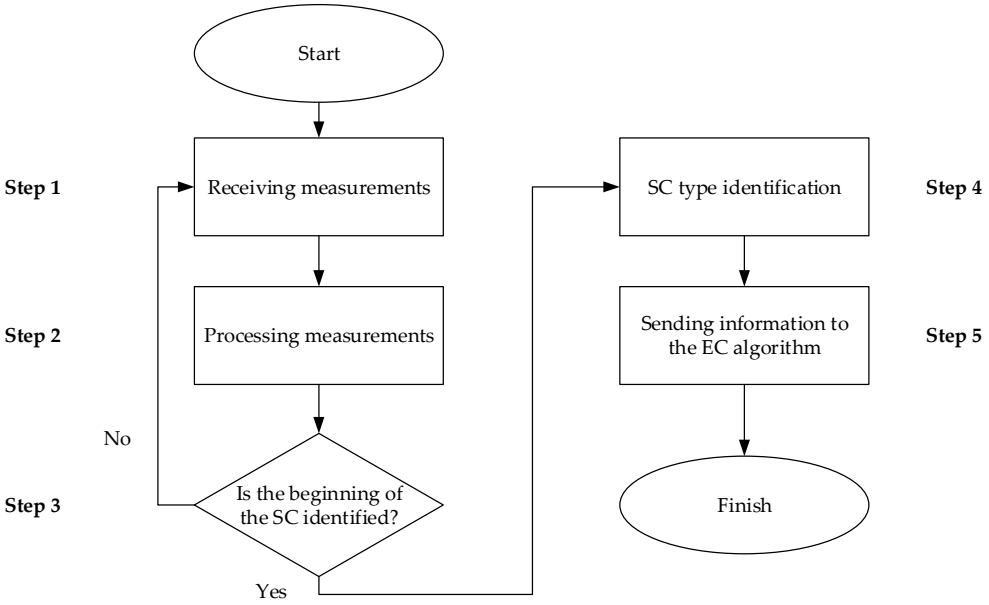


**Figure 3.** Flowchart of using a trained ML algorithm for EPS EC purposes.

The ML algorithm is trained using the following step-by-step technique:

Step 1: Data preparation, which involves generating a dataset consisting of results from transient process simulations in the EPS mathematical model and records of real-world transient events. Mathematical modeling enables the consideration of an extensive range of SCs across various electrical network configurations. However, this approach relies on model parameters that may differ significantly from actual system conditions [75,76]. In contrast, real data capture the true characteristics of transient processes for specific SCs, but its use is limited due to the unpredictability of SC frequency and parameters. By combining both sources, we ensure the dataset is both comprehensive and representative. The initial data consist of time series of current and voltage amplitudes and phases.

Step 2: Process the generated data sample in order to remove outliers, noise, perform correlation analysis of features in relation to classes and cross-correlation of features.

Step 3: Feature selection. This procedure is performed to reduce the dimensionality of the classification problem, which increases the speed of training and operation of the ML model [77–79]. Today, the following approaches are used for selecting features: filtering methods (chi-square test, Fisher test, correlation analysis); wrapper methods (direct feature selection, sequential feature selection, exhaustive feature selection, recursive feature exclusion); built-in methods (L1 regularization, methods based on the RF algorithm). The above feature selection methods are effective and are used in various applied data analysis problems. Built-in methods provide the greatest efficiency and speed of feature selection. Within the framework of international competitions in machine learning and the data analysis Kaggle [80], one of the most frequently used feature selection methods is Boruta [81,82]. This algorithm is based on the use of iterative training of the RF algorithm with sequential analysis of the Z-score of features.

Step 4: Training pre-selected ML models.

Step 5: Testing the trained ML models.

Step 6: Selecting the ML model with the best SC type classification accuracy.

During testing, the following quality metrics are calculated [31,32]:

$$Accuracy = \frac{TP + TN}{TP + TN + FP + FN}, \quad (1)$$

$$Precision = \frac{TP}{TP + FP}, \quad (2)$$

$$Recall = \frac{TP}{TP + FN} \quad (3)$$

$$F = \frac{2 \cdot PR \cdot RE}{PR + RE} \quad (4)$$

where *TP*—true positive responses, *TN*—true negative responses, *FP*—false positive responses, *FN*—false negative responses, *Accuracy*—SC type classification accuracy, *Precision*—proportion of correct model answers within the class, *Recall*—proportion true positive classifications, *F*—harmonic mean between *Precision* and *Recall*.

When using the trained ML algorithm for the purposes of emergency control of EPS modes, the block diagram is shown in Figure 2, the following computational steps are used:

Step 1: Obtaining measurements of the electrical parameters of the protected EPS.

Step 2: Processing measurements to remove outliers, noise, and missing data.

Step 3: If the onset of SC has been identified from the measurements obtained, then an assessment of the SC type is performed. Identification of the beginning of the SC can be performed by the accelerated method given in [83]. This accelerated algorithm is based on the analysis of the first derivative of the change in instantaneous values of currents and voltages over time.

Step 4: Identifying disturbance type using trained ML algorithm.

Step 5: Using SC type information in EPS EC.

To ensure redundancy of information, measurements for selected SC catches nearby to the location are used to identify the SC type.

Table 3 provides a description of each stage of the SC type determination procedure.

**Table 3.** Description of the stages of the SC type identification technique.

| № | Stage | Description |
|---|---|---|
| 1 | Preparation of initial data | Mathematical modeling data and real records of transient processes for the EPS under consideration are used. An accelerated algorithm is used to determine the amplitudes and phases of current and voltage signals [84]. |
| 2 | Data processing | Removal of outliers and filtering of high-frequency components in the amplitude and phase signals of currents and voltages. |
| 3 | Feature selection | Feature selection is carried out by the Boruta algorithm [81,82]. |
| 4 | Training ML algorithms | RF, AdaBoost, XGBoost, LightGBM were selected as the models under consideration. |
| 5 | Testing ML algorithms | Analysis of Accuracy, Precision, Recall, F values. |
| 6 | ML algorithm selection | The choice of model is made based on an analysis of quality metrics, as well as an analysis of performance. |

During the study, the block diagram shown in Figure 3 was not implemented in full due to the lack of a mathematical model for which there would be real data on transient processes. Therefore, the study was carried out in the following way: for the IEEE24 mathematical model [85,86], training and testing of ML models was carried out, an acceptable

model was selected in terms of accuracy and speed, an acceptable size of the calculation window and the sampling frequency of the original data were determined.

The next section provides testing of the proposed SC type identification method on synthetic and physical data, as well as an assessment of the acceptable measurement sampling frequency and the size of the calculation window of the synchrophasor evaluation method.

## 4. Case Study

To test the SC type identification technique, two types of data were used: synthetic data, generated using numerical modeling of transient processes in the IEEE24 model [85,86], and physical data obtained from PMUs installed at real power generation facilities. To take into account the influence of RES on determining the type and location of SC, three equivalent wind generators (WG) were added to the IEEE24 model and nodes 1, 2, and 3, simulating wind power plants.

### *4.1. Synthetic Data*

To generate the data sample, the standard IEEE24 mathematical model [85,86], implemented in Matlab Simulink, was used. The diagram of the IEEE24 model is shown in Figure 4, the parameters of synchronous generators (SG) are given in Table 4, the load parameters are presented in Table 5. The following notations are used in Table 4: $P_{ref}$—rated power, $x_d$ and $x_q$—synchronous resistance along the $d$ and axes $q$, $x_{d'}$ and $x_{q'}$—transition resistances along the $d$ and $q$ axes; in Table 5 the following designations are used: P and Q—active and reactive load of the node, $V_{max}$ and $V_{min}$—maximum and minimum voltage of the node in normal mode. Autotransformers and SGs were considered as grounding points. The SC impedances used were 0.1 p.u. for single-phase to ground SC, 0.2 p.u. for two-phase to ground SC, and 0.3 p.u. for phase-to-phase SC.

**Table 4.** Parameters of SGs used in the IEEE24 model.

| Generator | $P_{ref}$, MW | $x_d$, p.u. | $x_q$, p.u. | $x_d'$, p.u. | $x_q'$, p.u. |
|---|---|---|---|---|---|
| WG1 | 150 | – | – | – | – |
| WG2 | 150 | – | – | – | – |
| WG7 | 300 | – | – | – | – |
| SG13 | 600 | 0.254 | 0.241 | 0.050 | 0.081 |
| SG15 | 200 | 0.100 | 0.069 | 0.031 | 0.008 |
| SG16 | 150 | 0.262 | 0.285 | 0.043 | 0.166 |
| SG18 | 400 | 0.210 | 0.205 | 0.057 | 0.058 |
| SG21 | 400 | 0.210 | 0.205 | 0.057 | 0.058 |
| SG22 | 300 | 0.295 | 0.282 | 0.069 | 0.170 |
| SG23 | 300 | 0.295 | 0.282 | 0.069 | 0.170 |

To form a data sample, a mathematical modeling procedure was used with varying load levels in the nodes of the EPS mathematical model, location and type of SC, as well as the load level SG, ensuring the maintenance of power balance. Varying the loads in the nodes of the EPS mathematical model is performed by adding a random variable with a normal distribution with variance to the base loads of the nodes given in Table 5. The normal distribution is used taking into account the variance equal to 10% of the base load of the node.

The initial data are generated using a mathematical model of the EPS in Matlab Simulink. This includes a list of nodes where SC events are modeled, as well as the number of iterations involving load variations in the EPS nodes and single repairs of power lines. As the load changes, generation is adjusted to maintain the balance of active and reactive power within the EPS. Next, SC modeling is performed at selected EPS nodes and the results are recorded. When the cycles of changing loads in the EPS nodes and short-circuit modeling are completed, the algorithm is exited. The proposed algorithm can be parallelized in cycles of changing load levels and single repairs of power lines and enumerating nodes in which SC is modeled.

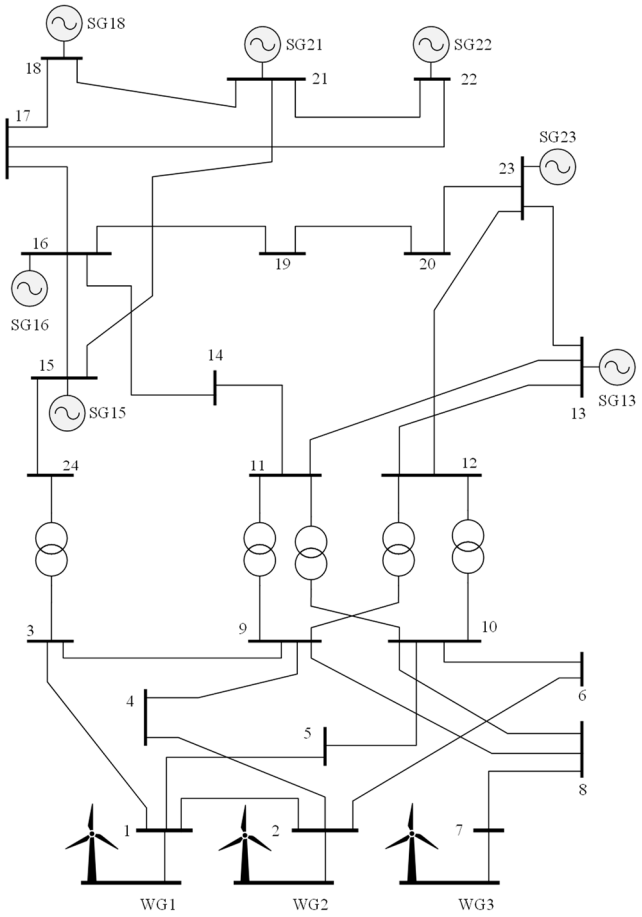


**Figure 4.** IEEE24 model diagram.

**Table 5.** Parameters of IEEE24 model nodes.

| Bus Number | P, MW | Q, MVAr | $V_{max}$, p.u. | $V_{min}$, p.u. |
|---|---|---|---|---|
| 1 | 108.0 | 22.0 | 1.05 | 0.95 |
| 2 | 97.0 | 20.0 | 1.05 | 0.95 |
| 4 | 74.0 | 15.0 | 1.05 | 0.95 |
| 5 | 71.0 | 14.0 | 1.05 | 0.95 |
| 6 | 136.0 | 28.0 | 1.05 | 0.95 |
| 9 | 175.0 | 36.0 | 1.05 | 0.95 |
| 13 | 265.0 | 54.0 | 1.05 | 0.95 |
| 15 | 317.0 | 64.0 | 1.05 | 0.95 |
| 16 | 100.0 | 20.0 | 1.05 | 0.95 |
| 18 | 333.0 | 68.0 | 1.05 | 0.95 |
| 20 | 128.0 | 26.0 | 1.05 | 0.95 |

Figure 5 shows graphs of changes in the active powers of WG1–WG3 depending on the number of the simulated electrical mode. Data from the study [87] were used to simulate the profile of change in active powers.

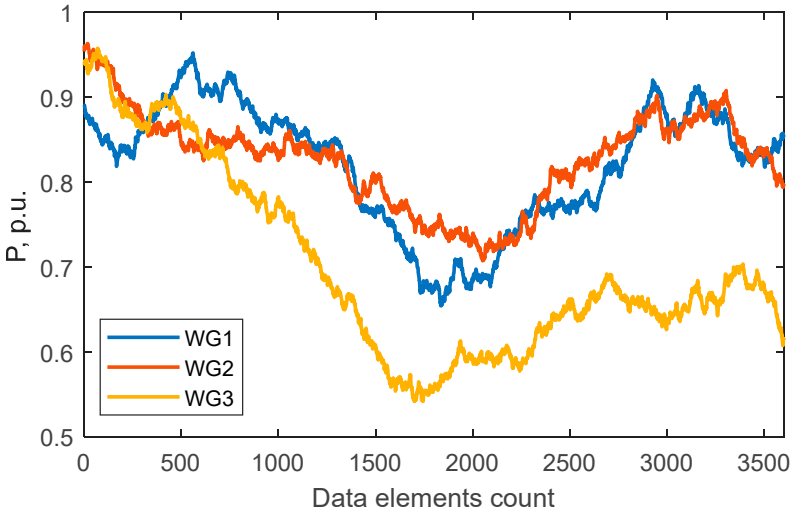


**Figure 5.** WG1–WG3 active powers.

The following data are used to identify the SC type:

- Amplitude and phase values of three voltage phases, determined for a given value of the sliding calculation window;
- Amplitude and phase values of three phases of currents of each connection, determined for a given value of the sliding calculation window;
- SC type (1—three-phase to ground, 2—phase-to-phase, 3—two-phase to ground, 4—single-phase to ground).

Table 6 presents the characteristics of the data sample. The table presents the number of SC types, SC duration, description of the features used in the data sample, number of transient processes, and distribution of transient process types for each class under consideration.

**Table 6.** Description of synthetic data sampling parameters.

| Characteristic | Value |
|---|---|
| Number of SC types | 4 |
| SC duration | 0.2 s |
| Features | Amplitude values of currents and voltages of phases A, B, and C, values of phase signals |
| Determining the list of nodes whose parameters are included in the data sample | According to Table 2 |
| Number of transients | 3600 |
| Number of transients in each class | 720—three-phase to ground SC<br>720—phase-to-phase SC<br>720—two-phase to ground SC<br>720—single-phase to ground SC<br>720—without SC |

To determine the parameters of instantaneous signals, the method presented in the study [84] was used. Figure 5 shows a fragment of the initial mathematical data: the instantaneous voltage signal of phase A and the calculated amplitude value in node 14, obtained during the simulation of a phase-to-phase SC in node 20 with a duration of 0.2 s. In Figure 6, the instantaneous voltage values of phase A are designated $u_a$, the amplitude values are designated $U_a$.

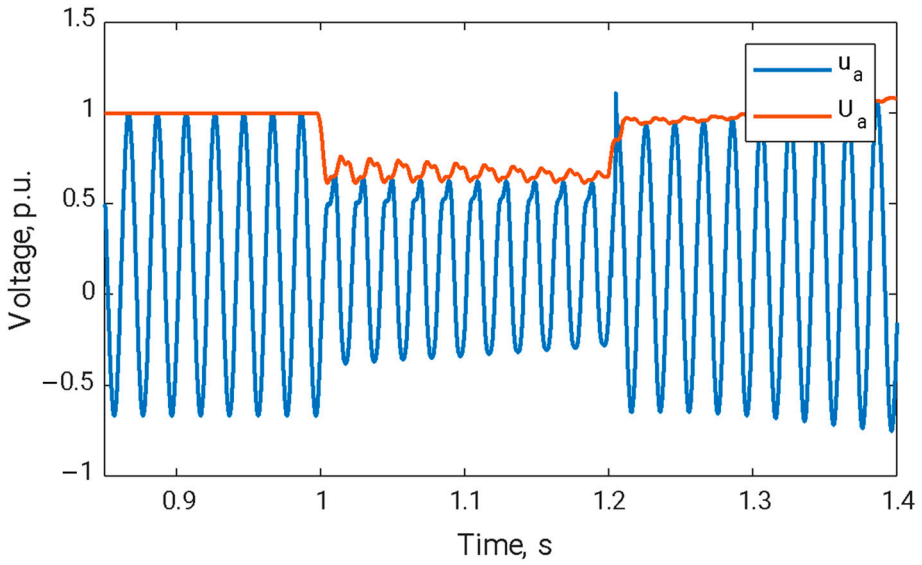


**Figure 6.** Fragment of initial mathematical data.

After forming a data sample, the stage of removing outliers and filtering high-frequency components in the signals of amplitudes and phases of currents and voltages is performed. For mathematical signals, this stage is not used, i.e., the IEEE24 model does not use the addition of noise and emissions characteristic of physical data.

To determine the significance of features, the Boruta algorithm [81,82] was used, applied to the original data sample. Table 7 presents the average values of the sign significance coefficients.

**Table 7.** Importance coefficients of data sample features.

| Feature | Importance |
|---|---|
| Phase A voltage module | 9.48 |
| Phase B voltage module | 9.43 |
| Phase C voltage module | 9.41 |
| Phase A current module | 12.85 |
| Phase B current module | 12.84 |
| Phase C current module | 12.88 |
| Voltage phase A | 2.15 |
| Voltage phase B | 2.11 |
| Voltage phase C | 2.21 |
| Current phase A | 3.17 |
| Current phase B | 3.19 |
| Current phase C | 3.15 |

The average value of the significance coefficients of phase amplitude signals is four times higher than the values of the significance coefficients of phase signals, which indicates the possibility of removing current and voltage phase signals from the data sample.

To train the RF, AdaBoost, XGBoost, and LightGBM algorithms, parameters were adjusted using the grid search method [88]. The total data sample was divided into testing and training with a ratio of 20/80%. Table 8 presents the optimal parameters obtained of each algorithm and classification quality metrics on the test dataset.

**Table 8.** Parameters of the considered ML algorithms and classification quality metrics on a test sample of synthetic data.

| Parameter | Value |
|---|---|
| RF | |
| n_estimators | 26 |
| max_depth | 7 |
| min_samples_split | 0.01 |
| min_samples_leaf | 0.01 |
| max_features | 2 |
| Accuracy | 85.3% |
| F | 82.4% |
| XGBoost | |
| n_estimators | 28 |
| max_depth | 6 |
| alpha | 0.04 |
| lambda | 0.04 |
| gamma | 1 |
| eta | 0,01 |
| learning_rate | 1 |
| Accuracy | 96.8% |
| F | 94.3% |
| AdaBoost | |
| n_estimators | 28 |
| learning_rate | 1 |
| Accuracy | 88.5% |
| F | 87.9% |
| LightGBM | |
| n_estimators | 20 |
| max_depth | 8 |
| alpha | 0.06 |
| lambda | 0.06 |
| num_leaves | 40 |
| learning_rate | 1 |
| Accuracy | 86.3% |
| F | 82.7% |

Table 8 uses the following notations: n_estimators—number of base classifiers, max_depth—depth of the base classifier tree, learning_rate—rate of gradient descent, min_samples_split—minimum number of data instances for splitting, min_samples_leaf—limit on the number of objects in leaves, max_features—maximum features for consideration within one base classifier, alpha—penalty for the values of weight functions in L1 regularization, lambda—penalty for the values of weight functions in L2 regularization, gamma—minimum required reduction in the loss function when creating a new sheet, eta—parameter weight compression to prevent overfitting, num_leaves—the maxi-

mum number of leaves of the base classifier tree. A detailed description of the algorithm parameters is given in the works: RF [89], XGBoost [90], AdaBoost [91], LightGBM [92]. Grid search was used to determine the optimal hyperparameters.

During the training process, after 40 iterations for all algorithms, steady-state values of the Accuracy and F coefficients were achieved, which varied within 70–100%, which indicates the determination of the optimal values of the algorithm parameters in the absence of retraining, which is expressed in 100% accuracy at training set.

When comparing the results of SC type classification on a test sample of synthetic data, the XGBoost algorithm achieved the highest values for both Accuracy and F-score. Additionally, it exhibited the fastest training speed among the algorithms tested.

### *4.2. Determination of the Acceptable Value of the Calculated Window for Synchrophasor Estimation and the Data Sampling Rate*

To determine the optimal calculation windows and data sampling rate, the XGBoost algorithm was repeatedly trained and tested by varying the sampling frequency from 20 kHz to 1 kHz in 1 kHz increments and adjusting the calculation window of the synchrophasor estimation algorithm [84] from 1 ms to 10 ms. Accuracy and F values were recorded during each iteration. The data sampling rate was modified using the decimation procedure. Acceptable parameters were identified through an analysis of the distributions of Accuracy and F values. Figure 7 illustrates the distribution of Accuracy, while Figure 8 shows the distribution of the F value. The legends in Figures 7 and 8 display the calculation window values of the synchrophasor estimation algorithm [84].

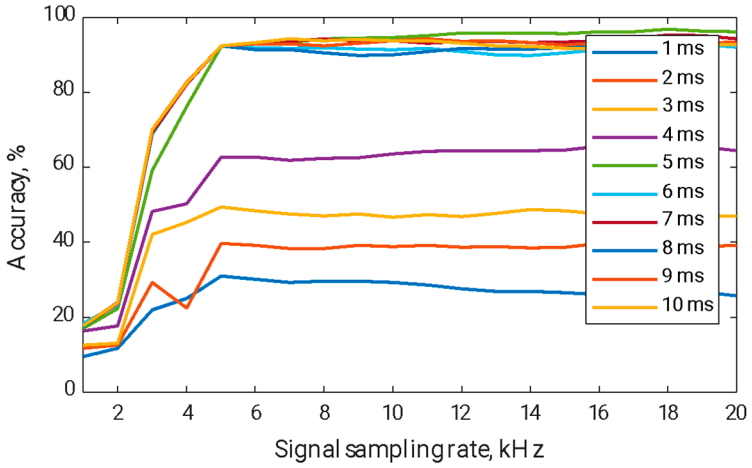


**Figure 7.** Distribution of the Accuracy value for the XGBoost algorithm when varying the size of the calculation window and the sampling frequency of the source data.

In the distributions of the Accuracy and F parameters, the so-called "long tail" phenomenon is observed when the calculation window reaches the value of 5 ms and a data sampling frequency of 5 kHz. When the values of the calculation window and sampling frequency increase above 5 ms and 5 kHz, the change in the Accuracy and F values does not exceed 2%. Therefore, for the considered SC with a duration of 0.2 s, these parameters are acceptable.

The values of the calculation window and the sampling frequency of the initial data are not strictly specified parameters; their determination can be performed when implementing the SC type identification algorithm. In this case, it is necessary to calculate the accuracy of synchrophasor estimation and SC type identification over a predetermined time interval to obtain characteristics similar to those shown in Figures 8 and 9. When obtaining these

characteristics, acceptable calculation windows and sampling frequencies can be obtained depending on the features of the analyzed signals.

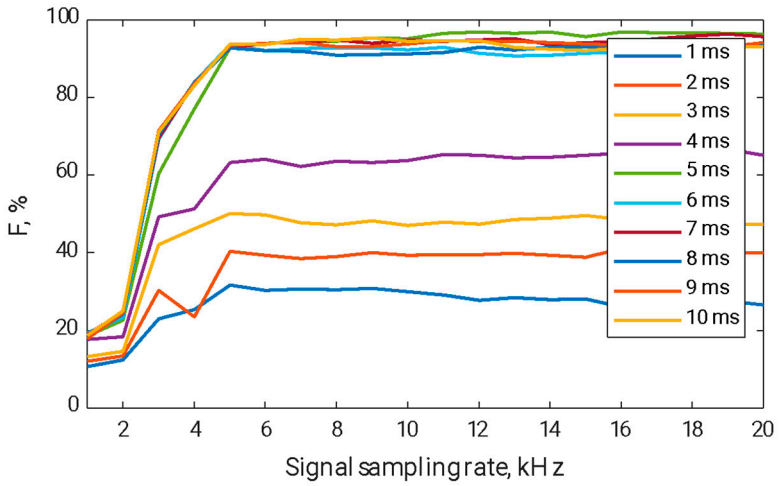


**Figure 8.** Distribution of the F value for the XGBoost algorithm when varying the size of the calculation window and the sampling frequency of the source data.

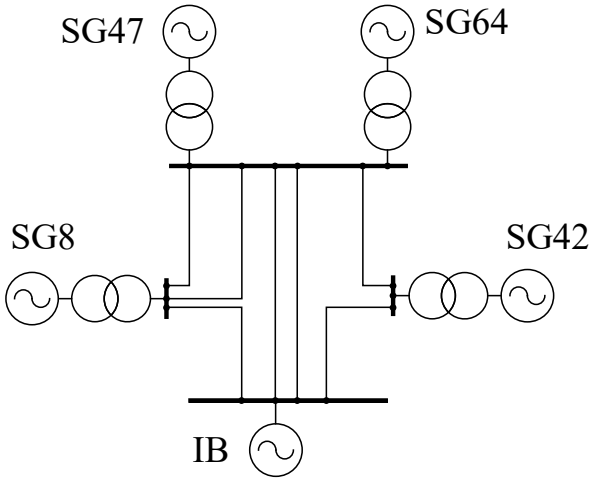


**Figure 9.** Diagram of the test physical system.

### *4.3. Physical Data*

To test the proposed SC type identification method, a physical model [93] was used, consisting of four SGs and infinite bus (IB), the connection diagram of which is shown in Figure 9. SG parameters are presented in Table 9.

**Table 9.** Parameters of SGs.

| Parameter | Value |
|---|---|
| SG 8 | |
| Rotor type | Salient-pole |
| Rated apparent capacity | 15 kVA |
| Power factor | 0.8 |
| Rated voltage | 230 V |
| Rated stator current | 37.5 A |
| Base impedance | 3.52 Ω |

**Table 9.** *Cont.*

| Parameter | Value |
|---|---|
| SG 42 | |
| Rotor type | Non-salient-pole |
| Rated apparent capacity | 5 kVA |
| Power factor | 0.8 |
| Rated voltage | 230 V |
| Rated stator current | 12.55 A |
| Base impedance | 10.58 Ω |
| SG 47 | |
| Rotor type | Non-salient-pole |
| Rated apparent capacity | 5 kVA |
| Power factor | 0.8 |
| Rated voltage | 230 V |
| Rated stator current | 12.55 A |
| Base impedance | 10.58 Ω |
| SG 64 | |
| Rotor type | Non-salient-pole |
| Rated apparent capacity | 5 kVA |
| Power factor | 0.8 |
| Rated voltage | 230 V |
| Rated stator current | 12.55 A |
| Base impedance | 10.58 Ω |

To test the proposed SC type identification technique, 200 SC records that occurred in the physical EPS model were selected. Signals of instantaneous phase currents and phase voltages were used as initial data. The SC type was determined by expert analysis of signal oscillograms. Table 10 shows the data sampling parameters.

**Table 10.** Description of physical data sampling parameters.

| Characteristic | Value |
|---|---|
| Number of SC types | 4 |
| SC duration | from 0.06 to 0.2 s |
| Features | Amplitude values of currents and voltages of phases A, B and C, phase signal values |
| Determining the list of nodes whose parameters are included in the data sample | According to Table 2 |
| Number of transients | 200 |
| Number of transients in each class | 40—three-phase to ground SC<br>40—phase-to-phase SC<br>40—two-phase to ground SC<br>40—single-phase to ground SC<br>40—without SC |

Figures 10 and 11 show snippets of the data used. Figure 10 shows instantaneous current signals, Figure 11 shows instantaneous voltage signals. The legends of Figures 10 and 11 show the designations of the phases of instantaneous signals.

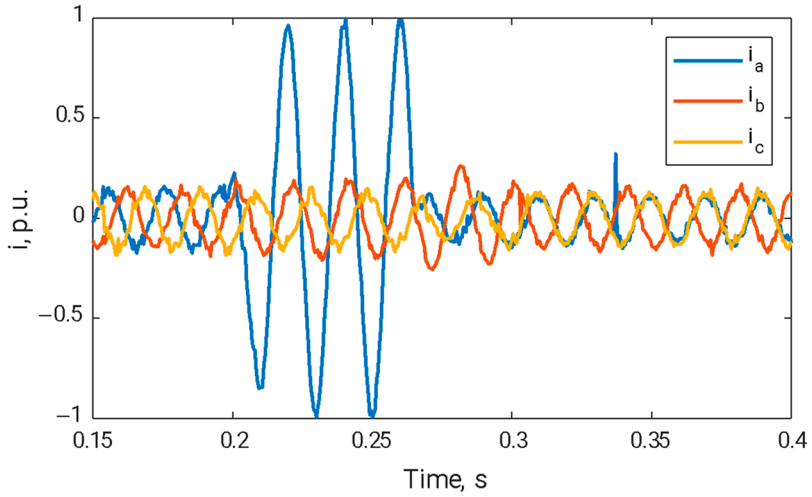


**Figure 10.** Instantaneous current signals.

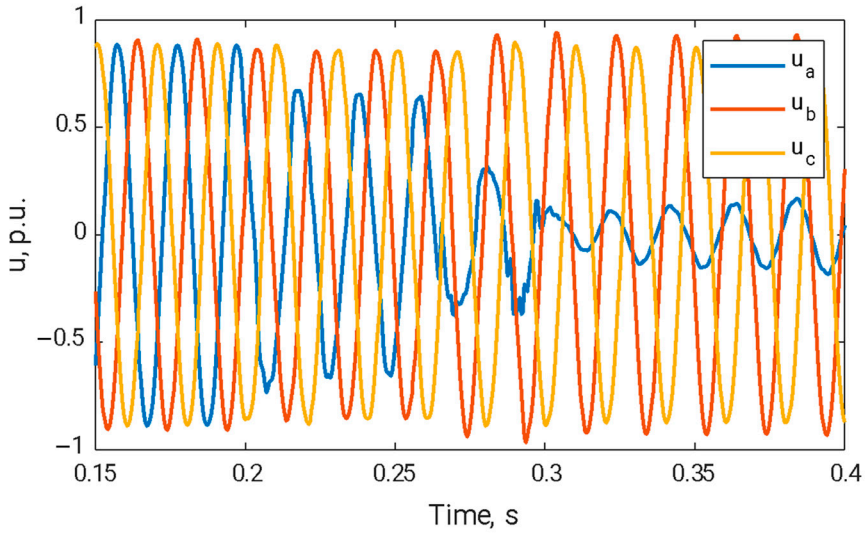


**Figure 11.** Instantaneous voltage signals.

The total data sample was divided into testing and training with the ratio of 20/80%. Table 11 presents the obtained optimal parameters of each algorithm and classification quality metrics on the test data sample. Table 11 uses symbols similar to those in Table 8.

**Table 11.** Parameters of the considered ML algorithms and classification quality metrics on a test sample of physical data.

| Parameter | Value |
|---|---|
| RF | |
| n_estimators | 20 |
| max_depth | 6 |
| min_samples_split | 0.01 |
| min_samples_leaf | 0.01 |
| max_features | 4 |
| Accuracy | 74.8% |
| F | 70.5% |

**Table 11.** *Cont.*

| Parameter | Value |
|---|---|
| XGBoost | |
| n_estimators | 20 |
| max_depth | 8 |
| alpha | 0.04 |
| lambda | 0.04 |
| gamma | 1 |
| eta | 0.01 |
| learning_rate | 1 |
| Accuracy | 85.2% |
| F | 83.4% |
| AdaBoost | |
| n_estimators | 30 |
| learning_rate | 1 |
| Accuracy | 64.1% |
| F | 62.6% |
| LightGBM | |
| n_estimators | 30 |
| max_depth | 9 |
| alpha | 0.06 |
| lambda | 0.06 |
| num_leaves | 60 |
| learning_rate | 1 |
| Accuracy | 79.5% |
| F | 78.4% |

When comparing the results of SC type classification on a test sample of physical data, the maximum values of the Accuracy and F coefficients correspond to the XGBoost algorithm, and the highest learning speed also corresponds to this algorithm.

The obtained results of SC classification on physical data differ from synthetic data in lower accuracy, which is associated with the following factors:

- Significant distortion of the shape of the curve of instantaneous currents and voltages obtained from the physical installation;
- Error in synchronization of measurements;
- Interference in the measuring system from electromagnetic fields caused by the proximity of high-voltage equipment to the place of measurements.

To overcome the identified shortcomings of testing on a physical model, it is necessary to consider signals from real EPS, for which the quality of measurements essentially exceeds measurements on a physical model. This section of the study will demonstrate the fundamental possibility of using the proposed approach to work in conditions of significant distortions of the initial data.

## 5. Discussion

The SC classification time delay is a critical value for EPS emergency control. The choice of control actions for maintaining TS in the post-emergency EPS operating mode is intended for the screw disconnection of the load or SG to prevent disturbance development. The speed of the transient process in EPS is determined by various factors such as: EPS

inertia, the presence of control devices based on power electronics, the correctness of the SG control system settings. The SC classification time delay makes the first contribution to the overall delay in TS assessment and decision-making regarding the need to introduce control in the EPS. In general, TS assessment is based on the analysis of differential equations describing the dynamic model of the protected EPS. In this system of equations, the smallest parameters are the time constants of automatic voltage control and power system stabilizers, which exceed the SC classification delay value of 5 ms determined in this study. Qualitatively, it can be stated that the SC classification delay value is acceptable for TS analysis. However, more accurate results can only be obtained through experiments using a real-time digital simulator.

## 6. Conclusions

One of the key features of modern EPS is the heightened demand for speed and adaptability in EC systems. The growing share of RES, along with advancements in digital control and monitoring systems, has altered the values of the inertial component, which influences the speed of transient processes. Consequently, the development of fundamentally new EC algorithms has become necessary [94].

In this study, an SC type identification technique was developed based on PMU data and ML algorithms. The proposed methodology was tested on synthetic and physical data. To generate the sample of synthetic data, the IEEE24 mathematical model was used, implemented in Matlab Simulink. The total volume of the synthetic data sample was 300 transient processes. The XGBoost algorithm achieved the highest classification accuracy for SC type in the synthetic data. For the physical data sample, changes derived from real EPS were applied. The total sample size consisted of 200 transients, with XGBoost again demonstrating the highest classification accuracy for SC type. Table 12 presents a comparison of the Accuracy and F coefficients for the ML algorithms considered in the SC type classification of both synthetic and physical data.

**Table 12.** Comparison of SC type classification results for synthetic and physical data.

| Algorithm | Synthetic Data | | Physical Data | |
|---|---|---|---|---|
| | Accyracy, % | F, % | Accyracy, % | F, % |
| RF | 85.3 | 82.4 | 74.8 | 70.5 |
| XGBoost | 96.8 | 94.3 | 85.2 | 83.4 |
| AdaBoost | 88.5 | 87.9 | 64.1 | 62.6 |
| LightGBM | 96.3 | 82.7 | 79.5 | 78.4 |

The study examined the issue of assessing the acceptable signal sampling frequency and the size of the calculation window of the method for synchrophasor estimation [84] for SC type classification. The following acceptable parameters of signal sampling frequency and calculation window size for SC type classification were determined: signal sampling frequency 5 kHz and calculation window size 5 ms.

The approach to SC type classification proposed in the article can be used for more complex EPS. In this case, SC type classification can be performed on several PDCs, and the final classification result can be obtained by averaging or a more complex data analysis procedure.

Future directions for research on this topic include the following:

- Consideration of large data samples generated for various EPS models, different short circuit durations, and the presence of power electronics devices in EPS models [95].
- Development of an algorithm for additional training of the model during operation.

- Determining the possibility of using ML algorithms to identify the type of SC using a real-time digital simulator [96].
- Application of the proposed method to remove noise from the raw data for other ML algorithms.
- The problem of identifying the entire spectrum of disturbances.
- Consideration of other ML methods for the problem of determining the type of SC (SVM, ANN, CNN, PNN, etc.).
- The issue of a detailed study of the possibility of using the proposed method for real signals.

**Author Contributions:** Conceptualization, M.S. (Mihail Senyuk) and F.K.; data curation, V.K.; formal analysis, I.Z., M.S. (Murodbek Safaraliev), and V.K.; investigation, M.S. (Mihail Senyuk) and S.B.; methodology, I.Z., M.S. (Murodbek Safaraliev), and S.B.; project administration, M.S. (Murodbek Safaraliev); resources, I.Z. and S.B.; software, M.S. (Mihail Senyuk), V.K. and F.K.; supervision, I.Z.; validation, M.S. (Mihail Senyuk) and F.K.; writing—original draft, M.S. (Mihail Senyuk), S.B. and V.K.; writing—review and editing, I.Z., M.S. (Murodbek Safaraliev), and F.K. All authors have read and agreed to the published version of the manuscript.

**Funding:** This research received no external funding.

**Data Availability Statement:** The original contributions presented in the study are included in the article material, further inquiries can be directed to the corresponding author.

**Acknowledgments:** The reported study was supported by Russian Science Foundation, research project № 23-79-01024.

**Conflicts of Interest:** The authors declare no conflicts of interest.

## Abbreviations

| | |
|---|---|
| AdaBoost | Adaptive boosting |
| ANN | Artificial neural network |
| CNN | Convolutional neural network |
| DFT | Discrete Fourier transform |
| DL | Deep learning |
| DT | Decision tree |
| DWT | Discrete wavelet transform |
| EC | Emergency control |
| EPS | Electric power system |
| FL | Fuzzy logic |
| IB | Infinite bus |
| KNN | K-nearest neighbors |
| LightGBM | Light gradient boosted machine |
| ML | Machine learning |
| PDC | Phasor data concentrator |
| PMU | Phasor measurement unit |
| PNN | Probabilistic neural network |
| RES | Renewable energy sources |
| RF | Random forest |
| SC | Short circuit |
| SG | Synchronous generator |
| SVM | Support vector machine |
| TS | Transient stability |
| XGBoost | Extreme gradient boosting |
| WG | Wind generator |

## References


1. Peyghami, S.; Palensky, P.; Blaabjerg, F. An Overview on the Reliability of Modern Power Electronic Based Power Systems. *IEEE Open J. Power Electron.* **2020**, *1*, 34–50. [CrossRef]
2. Cao, D.; Hu, W.; Zhao, J.; Zhang, G.; Zhang, B.; Liu, Z.; Chen, Z.; Blaabjerg, F. Reinforcement Learning and Its Applications in Modern Power and Energy Systems: A Review. *J. Mod. Power Syst. Clean Energy* **2020**, *8*, 1029–1042. [CrossRef]
3. Haegel, N.M.; Kurtz, S.R. Global Progress Toward Renewable Electricity: Tracking the Role of Solar (Version 2). *IEEE J. Photovolt.* **2022**, *12*, 1265–1272. [CrossRef]
4. Kroposki, B. Integrating high levels of variable renewable energy into electric power systems. *J. Mod. Power Syst. Clean Energy* **2017**, *5*, 831–837. [CrossRef]
5. Qazi, A.; Hussain, F.; Rahim, N.A.; Hardaker, G.; Alghazzawi, D.; Shaban, K.; Haruna, K. Towards Sustainable Energy: A Systematic Review of Renewable Energy Sources, Technologies, and Public Opinions. *IEEE Access* **2019**, *7*, 63837–63851. [CrossRef]
6. Zhou, Z.; Xiong, F.; Huang, B.; Xu, C.; Jiao, R.; Liao, B.; Yin, Z.; Li, J. Game-Theoretical Energy Management for Energy Internet With Big Data-Based Renewable Power Forecasting. *IEEE Access* **2017**, *5*, 5731–5746. [CrossRef]
7. Haegel, N.M.; Kurtz, S.R. Global Progress Toward Renewable Electricity: Tracking the Role of Solar. *IEEE J. Photovolt.* **2021**, *11*, 1335–1342. [CrossRef]
8. Zhang, Y.; Han, M.; Zhan, M. The Concept and Understanding of Synchronous Stability in Power Electronic-Based Power Systems. *Energies* **2023**, *16*, 2923. [CrossRef]
9. Yang, X.; Li, H.; Jia, W.; Liu, Z.; Pan, Y.; Qian, F. Adaptive Virtual Synchronous Generator Based on Model Predictive Control with Improved Frequency Stability. *Energies* **2022**, *15*, 8385. [CrossRef]
10. Alghamdi, A.S. A New Self-Adaptive Teaching–Learning-Based Optimization with Different Distributions for Optimal Reactive Power Control in Power Networks. *Energies* **2022**, *15*, 2759. [CrossRef]
11. Wu, Q.-H.; Bose, A.; Singh, C.; Chow, J.H.; Mu, G.; Sun, Y.; Liu, Z.; Li, Z.; Liu, Y. Control and Stability of Large-scale Power System with Highly Distributed Renewable Energy Generation: Viewpoints from Six Aspects. *CSEE J. Power Energy Syst.* **2023**, *9*, 8–14. [CrossRef]
12. Rao, H.; Wu, W.; Mao, T.; Zhou, B.; Hong, C.; Liu, Y.; Wu, X. Frequency control at the power sending side for large-scale HVDC asynchronous interconnection between Yunnan power grid and the rest of CSG. *CSEE J. Power Energy Syst.* **2020**, *7*, 105–113. [CrossRef]
13. Liu, H.; Bi, T.; Chang, X.; Guo, X.; Wang, L.; Cao, C.; Yan, Q.; Li, J. Impacts of subsynchronous and supersynchronous frequency components on synchrophasor measurements. *J. Mod. Power Syst. Clean Energy* **2016**, *4*, 362–369. [CrossRef]
14. Usman, M.U.; Faruque, M.O. Applications of synchrophasor technologies in power systems. *J. Mod. Power Syst. Clean Energy* **2018**, *7*, 211–226. [CrossRef]
15. Wang, G.; Guo, J.; Ma, S.; Zhang, X.; Guo, Q.; Fan, S.; Xu, H. Data-driven Transient Stability Assessment Using Sparse PMU Sampling and Online Self-check Function. *CSEE J. Power Energy Syst.* **2022**, *9*, 910–920. [CrossRef]
16. Phadke, A.G.; Bi, T. Phasor measurement units, WAMS, and their applications in protection and control of power systems. *J. Mod. Power Syst. Clean Energy* **2018**, *6*, 619–629. [CrossRef]
17. Senyuk, M.; Beryozkina, S.; Berdin, A.; Moiseichenkov, A.; Safaraliev, M.; Zicmane, I. Testing of an Adaptive Algorithm for Estimating the Parameters of a Synchronous Generator Based on the Approximation of Electrical State Time Series. *Mathematics* **2022**, *10*, 4187. [CrossRef]
18. Smolovik, S.V.; Koshcheev, L.A.; Lisitsyn, A.A.; Denisenko, A.I. Special Automation for Isolated Power Systems Emergency Control. In Proceedings of the 2021 IEEE Conference of Russian Young Researchers in Electrical and Electronic Engineering (ElConRus), St. Petersburg, Moscow, Russia, 26–29 January 2021; pp. 1558–1561. [CrossRef]
19. Gao, K.; Tian, C.; Fang, Z.; Cui, W.; Gao, Z.; Li, C. Optimal Control Time of Emergency Control to Damp Power System Low-Frequency. In Proceedings of the 2021 IEEE/IAS Industrial and Commercial Power System Asia (I&CPS Asia), Chengdu, China, 18–21 July 2021; pp. 704–709. [CrossRef]
20. Liu, G.; Shao, C.; Yan, Y.; Zhou, Z.; Xu, H.; Shi, Y.; Chen, X. Emergency Active Power Control Considering Power Reserve for Direct Driven Wind Power System Under Overspeed Power Shedding Operation. In Proceedings of the 2021 IEEE Sustainable Power and Energy Conference (iSPEC), Nanjing, China, 23–25 December 2021; pp. 3153–3158. [CrossRef]
21. Negnevitsky, M.; Voropai, N.; Kurbatsky, V.; Tomin, N.; Panasetsky, D. Development of an intelligent system for preventing large-scale emergencies in power systems. In Proceedings of the 2013 IEEE Power & Energy Society General Meeting, Vancouver, BC, Canada, 21–25 July 2013; pp. 1–5. [CrossRef]
22. Qie, Z.; Shi, Q.; Zhang, Z.; Li, Z.; Li, W.; Wang, W. Emergency Power Control Technology for Wind Power and Photovoltaic Power to Improve New Energy Consumption Capacity. In Proceedings of the 2019 IEEE 3rd Conference on Energy Internet and Energy System Integration (EI2), Changsha, China, 8–10 November 2019; pp. 2832–2837. [CrossRef]

23. Zhang, J.; Jiang, F.; Zhao, Y.; Chen, M.; Xin, H. An Improved Hierarchical and Decentralized Control Strategy for Emergency Power Supply During Disaster. In Proceedings of the 2018 International Conference on Power System Technology (POWERCON), Guangzhou, China, 6–8 November 2018; pp. 3485–3490. [CrossRef]
24. Rubasinghe, O.; Zhang, X.; Chau, T.K.; Chow, Y.H.; Fernando, T.; Iu, H.H.-C. A Novel Sequence to Sequence Data Modelling Based CNN-LSTM Algorithm for Three Years Ahead Monthly Peak Load Forecasting. *IEEE Trans. Power Syst.* **2023**, *39*, 1932–1947. [CrossRef]
25. Nose-Filho, K.; Lotufo, A.D.P.; Minussi, C.R. Short-Term Multinodal Load Forecasting Using a Modified General Regression Neural Network. *IEEE Trans. Power Deliv.* **2011**, *26*, 2862–2869. [CrossRef]
26. Prema, V.; Bhaskar, M.S.; Almakhles, D.; Gowtham, N.; Rao, K.U. Critical Review of Data, Models and Performance Metrics for Wind and Solar Power Forecast. *IEEE Access* **2021**, *10*, 667–688. [CrossRef]
27. Nabavi, S.A.; Motlagh, N.H.; Zaidan, M.A.; Aslani, A.; Zakeri, B. Deep Learning in Energy Modeling: Application in Smart Buildings With Distributed Energy Generation. *IEEE Access* **2021**, *9*, 125439–125461. [CrossRef]
28. Hong, T.; Pinson, P.; Wang, Y.; Weron, R.; Yang, D.; Zareipour, H. Energy Forecasting: A Review and Outlook. *IEEE Open Access J. Power Energy* **2020**, *7*, 376–388. [CrossRef]
29. Jeong, G.; Park, S.; Lee, J.; Hwang, G. Energy Trading System in Microgrids With Future Forecasting and Forecasting Errors. *IEEE Access* **2018**, *6*, 44094–44106. [CrossRef]
30. Khalyasmaa, A.I.; Valiev, R.T.; Bolgov, V.A. The methodology of risk evaluation for power equipment technical state assessment. In Proceedings of the 2017 15th International Conference on Electrical Machines, Drives and Power Systems (ELMA), Sofia, Bulgaria, 1–3 June 2017; pp. 493–496. [CrossRef]
31. Khalyasmaa, A.I.; Senyuk, M.D.; Eroshenko, S.A. Analysis of the State of High-Voltage Current Transformers Based on Gradient Boosting on Decision Trees. *IEEE Trans. Power Deliv.* **2020**, *36*, 2154–2163. [CrossRef]
32. Khalyasmaa, A.I.; Senyuk, M.D.; Eroshenko, S.A. High-Voltage Circuit Breakers Technical State Patterns Recognition Based on Machine Learning Methods. *IEEE Trans. Power Deliv.* **2019**, *34*, 1747–1756. [CrossRef]
33. Rao, T.S.M.; Anuradha, T.; Kaur, U.; Rajan, M.S.; Patnala, T.R.; Kumar, V.R. Machine Learning for the Assessment of Transient Stability of Power Systems. In Proceedings of the 2022 6th International Conference on Intelligent Computing and Control Systems (ICICCS), Madurai, India, 25–27 May 2022; pp. 1238–1242. [CrossRef]
34. Alimi, O.A.; Ouahada, K.; Abu-Mahfouz, A.M. A Review of Machine Learning Approaches to Power System Security and Stability. *IEEE Access* **2020**, *8*, 113512–113531. [CrossRef]
35. Shi, Z.; Yao, W.; Tang, Y.; Ai, X.; Wen, J.; Cheng, S. Bidirectional Active Transfer Learning for Adaptive Power System Stability Assessment and Dominant Instability Mode Identification. *IEEE Trans. Power Syst.* **2022**, *38*, 5128–5142. [CrossRef]
36. Zhao, T.; Yue, M.; Wang, J. Robust Power System Stability Assessment Against Adversarial Machine Learning-Based Cyberattacks via Online Purification. *IEEE Trans. Power Syst.* **2023**, *38*, 5613–5622. [CrossRef]
37. De Caro, F.; Collin, A.J.; Giannuzzi, G.M.; Pisani, C.; Vaccaro, A. Review of Data-Driven Techniques for On-Line Static and Dynamic Security Assessment of Modern Power Systems. *IEEE Access* **2023**, *11*, 130644–130673. [CrossRef]
38. Wang, X.Z.; Zhou, J.; Huang, Z.L.; Bi, X.L.; Ge, Z.Q.; Li, L. A multilevel deep learning method for big data analysis and emergency management of power system. In Proceedings of the 2016 IEEE International Conference on Big Data Analysis (ICBDA), Hangzhou, China, 12–14 March 2016; pp. 1–5. [CrossRef]
39. Huang, Q.; Huang, R.; Hao, W.; Tan, J.; Fan, R.; Huang, Z. Adaptive Power System Emergency Control Using Deep Reinforcement Learning. *IEEE Trans. Smart Grid* **2019**, *11*, 1171–1182. [CrossRef]
40. Zhang, K.; Zhang, J.; Xu, P.-D.; Gao, T.; Gao, D.W. Explainable AI in Deep Reinforcement Learning Models for Power System Emergency Control. *IEEE Trans. Comput. Soc. Syst.* **2021**, *9*, 419–427. [CrossRef]
41. Hossain, R.R.; Kumar, R. Machine Learning Accelerated Real-Time Model Predictive Control for Power Systems. *IEEE/CAA J. Autom. Sin.* **2023**, *10*, 916–930. [CrossRef]
42. Huang, R.; Chen, Y.; Yin, T.; Huang, Q.; Tan, J.; Yu, W.; Li, X.; Li, A.; Du, Y. Learning and Fast Adaptation for Grid Emergency Control via Deep Meta Reinforcement Learning. *IEEE Trans. Power Syst.* **2022**, *37*, 4168–4178. [CrossRef]
43. Zhu, L.; Luo, Y. Deep Feedback Learning Based Predictive Control for Power System Undervoltage Load Shedding. *IEEE Trans. Power Syst.* **2021**, *36*, 3349–3361. [CrossRef]
44. Morales-Hernandez, R.C.; Jaguey, J.G.; Becerra-Alonso, D. A Comparison of Multi-Label Text Classification Models in Research Articles Labeled With Sustainable Development Goals. *IEEE Access* **2022**, *10*, 123534–123548. [CrossRef]
45. Gulakhmadov, A.; Tavlintsev, A.; Pankratov, A.; Suvorov, A.; Kovaleva, A.; Lipnitskiy, I.; Safaraliev, M.; Semenenko, S.; Gubin, P.; Dmitriev, S.; et al. A Statistical-Based Approach to Load Model Parameter Identification. *IEEE Access* **2021**, *9*, 66915–66928. [CrossRef]
46. Razo-Hernandez, J.R.; Mejia-Barron, A.; Granados-Lieberman, D.; Valtierra-Rodriguez, M.; Gomez-Aguilar, J.F. A New Phasor Estimator for PMU Applications: P Class and M Class. *J. Mod. Power Syst. Clean Energy* **2020**, *8*, 55–66. [CrossRef]

47. Islam, Z.; Edib, S.N.; Vokkarane, V.M.; Lin, Y.; Fan, X. A Scalable PDC Placement Technique for Fast and Resilient Monitoring of Large Power Grids. *IEEE Trans. Control. Netw. Syst.* **2023**, *10*, 1770–1782. [CrossRef]
48. Bhattacharjee, R.; De, A. A Novel Bus-Ranking-Algorithm-Based Heuristic Optimization Scheme for PMU Placement. *IEEE Trans. Ind. Inform.* **2023**, *19*, 9921–9932. [CrossRef]
49. Kovalenko, P.Y. The extended frequency-directed EMD technique for analyzing the low-frequency oscillations in power systems. In Proceedings of the 2016 International Symposium on Industrial Electronics (INDEL), Banja Luka, Bosnia and Herzegovina, 17 January 2016; pp. 1–6. [CrossRef]
50. Majd, A.A.; Samet, H.; Ghanbari, T. k-NN based fault detection and classification methods for power transmission systems. *Prot. Control. Mod. Power Syst.* **2017**, *2*, 32. [CrossRef]
51. Venkata, P.; Pandya, V.; Vala, K.; Sant, A.V. Support vector machine for fast fault detection and classification in modern power systems using quarter cycle data. *Energy Rep.* **2022**, *8* (Suppl. S16), 92–98. [CrossRef]
52. Livani, H.; Evrenosoglu, C.Y. A Machine Learning and Wavelet-Based Fault Location Method for Hybrid Transmission Lines. *IEEE Trans. Smart Grid* **2013**, *5*, 51–59. [CrossRef]
53. Jena, M.K.; Tripathy, L.N.; Samantray, S.R. Intelligent relaying of UPFC based transmission lines using decision tree. In Proceedings of the 2013 1st International Conference on Emerging Trends and Applications in Computer Science, Shillong, India, 13–14 September 2013; pp. 224–229. [CrossRef]
54. Pradhan, A.; Routray, A.; Pati, S.; Pradhan, D. Wavelet Fuzzy Combined Approach for Fault Classification of a Series-Compensated Transmission Line. *IEEE Trans. Power Deliv.* **2004**, *19*, 1612–1618. [CrossRef]
55. Jamil, M.; Sharma, S.K.; Singh, R. Fault detection and classification in electrical power transmission system using artificial neural network. *SpringerPlus* **2015**, *4*, 334. [CrossRef]
56. Ramaswarny, S.; Kiran, B.; Kashyap, K.; Shen, U. Classification of power system transients using wavelet transforms and probabilistic neural networks. In Proceedings of the TENCON 2003. Conference on Convergent Technologies for Asia-Pacific Region, Bangalore, India, 15–17 October 2003; pp. 1272–1276. [CrossRef]
57. Chan, S.; Oktavianti, I.; Puspita, V.; Nopphawan, P. Convolutional Adversarial Neural Network (CANN) for Fault Diagnosis within a Power System: Addressing the Challenge of Event Correlation for Diagnosis by Power Disturbance Monitoring Equipment in a Smart Grid. In Proceedings of the 2019 International Conference on Information and Communications Technology (ICOIACT), Yogyakarta, Indonesia, 24–25 July 2019; pp. 596–601. [CrossRef]
58. Guo, M.-F.; Yang, N.-C.; Chen, W.-F. Deep-Learning-Based Fault Classification Using Hilbert–Huang Transform and Convolutional Neural Network in Power Distribution Systems. *IEEE Sens. J.* **2019**, *19*, 6905–6913. [CrossRef]
59. Fahim, S.R.; Sarker, S.K.; Muyeen, S.; Das, S.K.; Kamwa, I. A deep learning based intelligent approach in detection and classification of transmission line faults. *Int. J. Electr. Power Energy Syst.* **2021**, *133*, 107102. [CrossRef]
60. Parthasarathy, G.; Chatterji, B. A class of new KNN methods for low sample problems. *IEEE Trans. Syst. Man Cybern.* **1990**, *20*, 715–718. [CrossRef]
61. Scholkopf, B.; Sung, K.-K.; Burges, C.; Girosi, F.; Niyogi, P.; Poggio, T.; Vapnik, V. Comparing support vector machines with Gaussian kernels to radial basis function classifiers. *IEEE Trans. Signal Process.* **1997**, *45*, 2758–2765. [CrossRef]
62. Tsang, S.; Kao, B.; Yip, K.Y.; Ho, W.-S.; Lee, S.D. Decision Trees for Uncertain Data. *IEEE Trans. Knowl. Data Eng.* **2009**, *23*, 64–78. [CrossRef]
63. Hu, Q.; Che, X.; Zhang, L.; Zhang, D.; Guo, M.; Yu, D. Rank Entropy-Based Decision Trees for Monotonic Classification. *IEEE Trans. Knowl. Data Eng.* **2011**, *24*, 2052–2064. [CrossRef]
64. Manwani, N.; Sastry, P.S. Geometric Decision Tree. *IEEE Trans. Syst. Man Cybern. Part B (Cybern.)* **2011**, *42*, 181–192. [CrossRef] [PubMed]
65. Jang, J.-S.R.; Sun, C.-T. Neuro-fuzzy modeling and control. *Proc. IEEE* **1995**, *83*, 378–406. [CrossRef]
66. Yao, X. Evolving artificial neural networks. *Proc. IEEE* **1999**, *87*, 1423–1447. [CrossRef]
67. Guillod, T.; Papamanolis, P.; Kolar, J.W. Artificial Neural Network (ANN) Based Fast and Accurate Inductor Modeling and Design. *IEEE Open J. Power Electron.* **2020**, *1*, 284–299. [CrossRef]
68. Jinia, A.J.; Maurer, T.E.; Meert, C.A.; Hua, M.Y.; Clarke, S.D.; Kim, H.-S.; Wentzloff, D.D.; Pozzi, S.A. An Artificial Neural Network System for Photon-Based Active Interrogation Applications. *IEEE Access* **2021**, *9*, 119871–119880. [CrossRef]
69. Madvar, H.R.; Dehghani, M.; Memarzadeh, R.; Salwana, E.; Mosavi, A.; Shahab, S. Derivation of Optimized Equations for Estimation of Dispersion Coefficient in Natural Streams Using Hybridized ANN With PSO and CSO Algorithms. *IEEE Access* **2020**, *8*, 156582–156599. [CrossRef]
70. Devyatkin, D.A.; Grigoriev, O.G. Random Kernel Forests. *IEEE Access* **2022**, *10*, 77962–77979. [CrossRef]
71. Wu, S.; Nagahashi, H. Parameterized AdaBoost: Introducing a Parameter to Speed Up the Training of Real AdaBoost. *IEEE Signal Process. Lett.* **2014**, *21*, 687–691. [CrossRef]
72. Li, N.; Li, B.; Gao, L. Transient Stability Assessment of Power System Based on XGBoost and Factorization Machine. *IEEE Access* **2020**, *8*, 28403–28414. [CrossRef]

73. Min, F.; Yaling, L.; Xi, Z.; Huan, C.; Yaqian, H.; Libo, F.; Qing, Y. Fault prediction for distribution network based on CNN and LightGBM algorithm. In Proceedings of the 2019 14th IEEE International Conference on Electronic Measurement & Instruments (ICEMI), Changsha, China, 1–3 November 2019; pp. 1020–1026. [CrossRef]
74. Mienye, I.D.; Sun, Y. A Survey of Ensemble Learning: Concepts, Algorithms, Applications, and Prospects. *IEEE Access* **2022**, *10*, 99129–99149. [CrossRef]
75. Moiseichenkov, A.N.; Kovalenko, P.Y.; Senyuk, M.D.; Mukhin, V.I. Synchronous Machine Adaptive Model for Power System Emergency Control and Technical State Diagnostic. In Proceedings of the 2020 Ural Smart Energy Conference (USEC), Ekaterinburg, Russia, 13–15 November 2020; pp. 147–150. [CrossRef]
76. Zhou, Y.; She, J.; Ryuichi, Y. Branch Parameter Estimation for Aging Power System Using System Identification Theory. In Proceedings of the 2023 13th International Conference on Power, Energy and Electrical Engineering (CPEEE), Tokyo, Japan, 25–27 February 2023; pp. 97–100. [CrossRef]
77. Zhou, P.; Li, P.; Zhao, S.; Wu, X. Feature Interaction for Streaming Feature Selection. *IEEE Trans. Neural Netw. Learn. Syst.* **2020**, *32*, 4691–4702. [CrossRef] [PubMed]
78. Thabtah, F.; Kamalov, F.; Hammoud, S.; Shahamiri, S.R. Least Loss: A simplified filter method for feature selection. *Inf. Sci.* **2020**, *534*, 1–15. [CrossRef]
79. Kamalov, F.; Sulieman, H.; Moussa, S.; Reyes, J.A.; Safaraliev, M. Nested ensemble selection: An effective hybrid feature selection method. *Heliyon* **2023**, *9*, e19686. [CrossRef]
80. Yang, X.; Ding, J. A Computational Framework for Iceberg and Ship Discrimination: Case Study on Kaggle Competition. *IEEE Access* **2020**, *8*, 82320–82327. [CrossRef]
81. Malallah, O.M. Handwritten Signature Forgery Detection Using PCA and Boruta Feature Selection. In Proceedings of the 2022 4th International Conference on Advanced Science and Engineering (ICOASE), Zakho, Iraq, 21–22 September 2022; pp. 160–165. [CrossRef]
82. Kavitha, K.R.; Sajith, S.; Variar, N.H. An Efficient Boruta-Based Feature Selection and Classification of Gene Expression Data. In Proceedings of the 2022 IEEE 3rd Global Conference for Advancement in Technology (GCAT), Bangalore, India, 7–9 October 2022; pp. 1–6. [CrossRef]
83. Senyuk, M.; Beryozkina, S.; Gubin, P.; Dmitrieva, A.; Kamalov, F.; Safaraliev, M.; Zicmane, I. Fast Algorithms for Estimating the Disturbance Inception Time in Power Systems Based on Time Series of Instantaneous Values of Current and Voltage with a High Sampling Rate. *Mathematics* **2022**, *10*, 3949. [CrossRef]
84. Beryozkina, S.; Senyuk, M.; Berdin, A.; Dmitrieva, A.; Dmitriev, S.; Erokhin, P. The Accelerate Estimation Method of Power System Parameters in Static and Dynamic Processes. *IEEE Access* **2022**, *10*, 61522–61529. [CrossRef]
85. Niu, R.; Zeng, Y.; Cheng, M.; Wang, X. Study on load-shedding model based on improved power flow tracing method in power system risk assessment. In Proceedings of the 2011 4th International Conference on Electric Utility Deregulation and Restructuring and Power Technologies (DRPT), Weihai, China, 6–9 July 2011; pp. 45–50. [CrossRef]
86. Lukacevic, O.; Calasan, M.; Mujovic, S. Impact of optimal ESS allocation in IEEE 24-test bus system on total production cost. In Proceedings of the 2019 20th International Symposium on Power Electronics (Ee), Novi Sad, Serbia, 23–26 October 2019; pp. 1–5. [CrossRef]
87. Derviskadic, A.; Zuo, Y.; Frigo, G.; Paolone, M. Under Frequency Load Shedding based on PMU Estimates of Frequency and ROCOF. In Proceedings of the 2018 IEEE PES Innovative Smart Grid Technologies Conference Europe (ISGT-Europe), Sarajevo, Bosnia and Herzegovina, 21–25 October 2018; pp. 1–6. [CrossRef]
88. Lin, J.; Zhang, J. A Fast Parameters Selection Method of Support Vector Machine Based on Coarse Grid Search and Pattern Search. In Proceedings of the 2013 Fourth Global Congress on Intelligent Systems, Hong Kong, China, 3–4 December 2013; pp. 77–81. [CrossRef]
89. Geurts, P.; Ernst, D.; Wehenkel, L. Extremely randomized trees. *Mach. Learn.* **2006**, *63*, 3–42. [CrossRef]
90. Chen, T.; Guestrin, C. XGBoost: A Scalable Tree Boosting System. In Proceedings of the 22nd ACM SIGKDD International Conference on Knowledge Discovery and Data Mining (KDD'16), San Francisco, CA, USA, 13–17 August2016; Association for Computing Machinery: New York, NY, USA, 2016; pp. 785–794. [CrossRef]
91. Mekhalfa, F.; Nacereddine, N. Gentle Adaboost algorithm for weld defect classification. In Proceedings of the 2017 Signal Processing: Algorithms, Architectures, Arrangements, and Applications (SPA), Poznan, Poland, 20–22 September 2017; pp. 301–306. [CrossRef]
92. Machado, M.R.; Karray, S.; de Sousa, I.T. LightGBM: An Effective Decision Tree Gradient Boosting Method to Predict Customer Loyalty in the Finance Industry. In Proceedings of the 2019 14th International Conference on Computer Science & Education (ICCSE), Toronto, ON, Canada, 19–21 August 2019; IEEE: Toronto, ON, Canada, 2019; pp. 1111–1116. [CrossRef]
93. Kovalenko, P.Y.; Moiseichenkov, A.N. Comparing the techniques of defining the synchronous machine load angle. *J. Phys. Conf. Ser.* **2017**, *870*, 012013. [CrossRef]

94. Senyuk, M.; Beryozkina, S.; Safaraliev, M.; Pazderin, A.; Odinaev, I.; Klassen, V.; Savosina, A.; Kamalov, F. Bulk Power Systems Emergency Control Based on Machine Learning Algorithms and Phasor Measurement Units Data: A State-of-the-Art Review. *Energies* **2024**, *17*, 764. [CrossRef]
95. Senyuk, M.; Safaraliev, M.; Pazderin, A.; Pichugova, O.; Zicmane, I.; Beryozkina, S. Methodology for Power Systems' Emergency Control Based on Deep Learning and Synchronized Measurements. *Mathematics* **2023**, *11*, 4667. [CrossRef]
96. Kuffel, R.; Giesbrecht, J.; Maguire, T.; Wierckx, R.; McLaren, P. RTDS-a fully digital power system simulator operating in real time. In Proceedings of the IEEE WESCANEX Communications, Power, and Computing, Winnipeg, MB, Canada, 21–23 November 1995; pp. 300–305. [CrossRef]